Supporting Information

A Hydrolyzable Quaternary Ammonium Bactericide with Charge-Shielding-Assisted Detoxification

Jiahao Huang, An Zhang, Wenwen Han, Xiao-Qi Xu, Bin Yuan, Xu Yan and Yapei Wang*

School of Chemistry and Life Resources, Renmin University of China, Beijing 100872, China

*Corresponding author: yapeiwang@ruc.edu.cn (Yapei Wang)

Contents

Note S1. Materials.

N,N-dimethyldecamine, N, N-dimethyldodecylamine, N, N-dimethyltetradecylamine, N,N-Dimethylhexadecylamine, methyl bromoacetate, ethyl bromoacetate, tert butyl bromoacetate and DMSO-d_6 were purchased from Shanghai Meryer Biochemical Technology Co., Ltd. (Beijing China). Chromatographic grade methanol, anhydrous ether, sodium hydroxide and anhydrous potassium bromide (KBr) were purchased from Sinopharm Chemical Reagent Co., Ltd. (Shanghai, China). 4,4'-Bipyridine was purchased from Shanghai Energy Chemicals Co., Ltd. (Shanghai, China). Dimethyl formamide (DMF), dimethyl sulfoxide (DMSO), diethyl ether, acetonitrile and methylene chloride were purchased from Beijing Tong Guang Fine Chemicals Company (Beijing, China). 2',7'-dichlorodihydrofluorescein diacetate (DCFH-DA) were purchased from Shanghai Aladdin Biochemical Technology Co., Ltd. (Shanghai, China). All chemicals were directly used without further purification. Dulbecco's modified eagle medium (DMEM) was obtained from Cytiva (Marlborough, Middlesex, MA, United States). Phosphate buffered solution (PBS) was obtained from Biotopped (Beijing, China). The cell counting kit-8 (CCK-8, C0038) reagent, Calcein-AM/propidium iodide cell viability assay kit (C2015S) and ROS Assay Kit (S0033M) were purchased from Beyotime Biotechnology Co., Ltd. Escherichia coli (CICC 10899, revived), and Staphylococcus aureus (CICC 21600, revived) were obtained from China Center of Industrial Culture Collection (Beijing, China). Staphylococcus aureus (MRSA, ATCC 43300) and carbapenem-resistant Escherichia coli (CREC, clinical isolate) were recovered from clinical specimens in Beijing Friendship Hospital during January 2018 and May 2023 (Beijing, China). The culture medium of bacteria Luria-Bertani broth, nutrient agar, and Mueller-Hinton broth were purchased from Beijing Aoboxing Bio-Tech Co., Ltd. (Beijing, China) and used after being sterilized in an autoclave at 121 °C for 20 min. Mouse epithelioid fibroblast cell L929 was cultured in Dulbecco's Modified Eagle Medium purchased from Cytiva Co., Ltd. (Shanghai, China) containing 10% fetal bovine serum (FBS) and 1% penicillin/streptomycin. Deionized water was obtained by a Milli-Q water purification system.

Note S2. Characterization.

The ^{1}H NMR was recorded on a Bruker AVANCE 400 MHz spectrometer in D_2O. High-resolution mass spectra (HRMS) were acquired on a Thermo Q-Exactive instrument (quadrupole mass analyzer) using an atmospheric pressure chemical ionization source (APCI). The FTIR spectra were obtained through a CaF_2 optical window, with a Bruker TENSOR 27. All UV-Vis-NIR spectra were measured on a Shimadzu UV-3600 spectrometer with a temperature control attachment (Shimadzu Corp., Kyoto, Japan). Fluorescent images of cells stained by DCFH-DA were captured by the laser scanning confocal fluorescence microscope (TCS SP8, Leica, Wetzlar, Germany). Fluorescent images of cells stained by Calcein-AM/propidium iodide (PI) and DCFH-DA were acquired using a Nikon Ti2-E inverted fluorescence microscope (Nikon Corporation, Tokyo, Japan). The temperature was monitored using a K-type thermocouple (TT-K-30-SLE, Omega Engineering Inc., Stamford, CT, USA). The photographs were captured using a Canon EOS 70D camera (Canon Inc., Tokyo, Japan). The pH of the solutions was measured using a Radiometer pH meter (Radiometer, Copenhagen, Denmark). The optical absorption of the formazan dye at 450 nm in the cellular cytotoxicity experiment was detected by an EPOCH2 microplate spectrophotometer (BioTek Instruments Inc., Winooski, VT, United States). Zeta potential measurements were conducted using a Zetasizer Nano ZS series instrument (Malvern Panalytical, UK). Isothermal Titration Calorimetry (ITC) measurements were performed using a PEAQ-ITC instrument (Malvern Panalytical, UK). Scanning Electron Microscopy (SEM) were conducted using a Sigma 300 microscope (Carl Zeiss, Germany). High-Performance Liquid Chromatography (HPLC) was performed using an Agilent 1260 Infinity II HPLC system (Agilent Technologies, USA) equipped with a quaternary pump, an autosampler, a thermostated column compartment, and a diode array detector (DAD).

Note S3. Experimental methods.

The Synthesis of Ester-Functionalized Quaternary Ammonium Salts (Cn-N-R).

A series of ester-quaternary ammonium compounds (Ester-QACs) with varying alkyl chain lengths and ester groups were synthesized via a one-step quaternization reaction. Typically, C_{16}-N-Me was synthesized as a representative example. N,N-Dimethylhexadecylamine (2.96 g, 0.011 mol) and methyl bromoacetate (1.53 g, 0.01 mol) were dissolved in 20 mL of anhydrous diethyl ether in a round-bottom flask. The reaction mixture was stirred magnetically at a constant temperature of 30 °C for 6 hours. During this period, a white solid precipitated from the solution. The resulting solid was collected and subsequently washed with fresh anhydrous diethyl ether five times via centrifugation to remove any unreacted starting materials. The final product was dried under vacuum at room temperature for 24 hours to yield a pure white solid. The other Ester-QACs (e.g., Cn-N-R, where n = 10, 12, 14, 16, R = Me, Et, t-Bu) were synthesized analogously by employing the corresponding N,N-dimethylalkylamine and bromoacetate ester. All compounds were obtained in excellent and consistent yields ranging from 90% to 94%.

The Synthesis of Hydrolyzed Products (Cn-N-Na)

The hydrolyzed products, sodium carboxylate salts (Cn-N-Na), were synthesized by the basic hydrolysis of the corresponding ester-quaternary ammonium compounds (Ester-QACs). Using the hydrolysis of C_{16}-N-Me to C_{16}-N-Na as a representative example: The precursor C_{16}-N-Me (1.0 g) was suspended in 30 mL water. The suspension was stirred and heated to 30 °C to facilitate dissolution. Aqueous sodium hydroxide (NaOH, 1 M) was then added dropwise to the stirred solution until the pH was stably maintained at 10. The reaction mixture was stirred continuously at 30 °C for 12 hours to ensure complete hydrolysis. Upon completion, the solvent was removed under reduced pressure. The resulting crude solid was thoroughly washed with cold anhydrous ethanol and dried under vacuum to afford C_{16}-N-Na as a white, hygroscopic powder. The hydrolysis of other Ester-QACs (Cn-N-R) to their respective Cn-N-Na salts was performed using this analogous procedure.

^{1}H NMR Characterization of Ester-QACs (Cn-N-R)

Approximately 10-15 mg of the purified Ester-QAC compound was accurately weighed and dissolved in 0.6 mL of deuterated dimethyl sulfoxide (DMSO-d_6). The solution was transferred to a standard 5 mm NMR tube for analysis. All spectra were acquired at room temperature. Chemical shifts (δ) are reported in parts per million (ppm) and are referenced relative to the residual DMSO solvent peak at 2.50 ppm.

MS Characterization of Ester-QACs (Cn-N-R)

The sample was prepared by dissolving approximately 1 mg of the purified Ester-QAC compound in 1 mL of a methanol/water (1:1, v/v) mixture. The solution was further diluted with the same solvent mixture to a final concentration of approximately 1-10 μg/mL prior to injection. The analysis was performed in positive ion mode.

FT-IR Spectroscopy of Ester-QACs (Cn-N-R)

Approximately 1-2 mg of the purified, dry Ester-QAC solid was carefully mixed with 200 mg of anhydrous potassium bromide (KBr, spectroscopic grade) in an agate mortar and ground thoroughly to form a fine, homogeneous powder. The mixture was then transferred into a pellet die and pressed under a hydraulic press under a pressure of 10-15 tons for 2-3 minutes to form a transparent pellet. Spectra were acquired over a wavenumber range of 4000 to 400 cm^{-1} with a resolution of 4 cm^{-1}. Each spectrum represents the average of 32 scans to ensure a high signal-to-noise ratio. A background spectrum of a pure KBr pellet was collected and automatically subtracted by the instrument software prior to sample measurement.

In Situ ^{1}H NMR Monitoring of Hydrolysis Kinetics for Ester-QACs (Cn-N-R)

A stock solution of the Ester-QAC (Cn-N-R) was prepared in deuterated water (D_2O) at a concentration of 10 mM. To study pH-dependent kinetics, the pD of the D_2O stock solution was adjusted using NaOD or DCl. The desired pD values were thus calibrated accordingly. For each kinetic run, 0.6 mL of the prepared stock solution was transferred to a standard 5 mm NMR tube. The NMR tube was then placed into the spectrometer's probe, which was pre-equilibrated to the target temperature. A series of ^{1}H NMR spectra were acquired automatically at predetermined time intervals over the course of the reaction. The acquisition of the first spectrum was defined as time zero (t = 0).

Zeta Potential Measurements for Probing Dynamic Electrostatic Interactions

Zeta potential measurements were employed to monitor in real-time the dynamic electrostatic interaction between the model compound Cn-N-R and the cell envelopes of Escherichia coli (E. coli) and Staphylococcus aureus (S. aureus). Both bacterial strains were cultured overnight in Luria-Bertani (LB) broth at 37 ºC with shaking at 200 rpm. The cells were harvested in the mid-logarithmic growth phase by centrifugation (5000 × g, 10 min, 4 ºC) and washed twice with sterile, isotonic phosphate-buffered saline (PBS, 1X, pH 7.4). The final bacterial pellets were resuspended in PBS to an optical density at 600 nm (OD_{600}) of approximately 0.5, corresponding to a cell density of ~10^8 CFU/mL, to ensure optimal measurement conditions. 1 mL of the prepared bacterial suspension was transferred into a disposable zeta potential cell. The zeta potential of the untreated bacteria was measured first to establish the baseline value. All measurements were performed at 25 ºC. A concentrated stock solution of C_{16}-N-Me in PBS was spiked directly into the bacterial suspension in the measurement cell to achieve a final concentration of 0.5mM. The suspension was mixed by gentle pipetting for 10 seconds. The zeta potential was measured immediately after mixing (within 1-2 minutes) to capture the initial binding event. The measurement cell was then left undisturbed in the instrument. Repeat the above operation at regular intervals within 60 hours to measure the zeta potential after hydrolysis, in order to track the changes in C_{16}-N-Me hydrolysis in PBS aqueous buffer.

Isothermal Titration Calorimetry (ITC) with Bacterial Membrane Vesicles

Both bacterial strains were cultured in 1 L of LB broth at 37 °C with shaking (200 rpm) until the mid-logarithmic phase. Cells were harvested by centrifugation (6000 × g, 15 min, 4 °C). The cell pellets were washed and resuspended in 30 mL of ice-cold lysis buffer (20 mM Tris-HCl, pH 7.5, containing 150 mM NaCl, 1 mM EDTA, and one tablet of EDTA-free protease inhibitor cocktail). Cells were disrupted on ice using an ultrasonic cell disruptor equipped with a tapered microtip. The suspension was subjected to pulsed sonication (5 seconds on, 10 seconds off) at an amplitude of 30-40% for a total process time of 5-10 minutes, ensuring the sample tube was immersed in an ice-water bath throughout the procedure to prevent overheating. The lysate was first centrifuged at 5,000 × g for 15 min at 4 °C to remove unbroken cells and debris. The

resulting supernatant was then subjected to ultracentrifugation at 150000 × g for 1 hour at 4 °C to pellet the total membrane fraction. The membrane pellet was gently washed and resuspended in a minimal volume of ITC assay buffer (20 mM Tris-HCl, pH 7.5, 150 mM NaCl). The titrant (C_{16}-N-Me or C_{16}-N-Na) was dissolved in the ITC assay buffer to a final concentration of 2 mM. The membrane vesicle suspension was used as the sample in the cell. Measurements were performed on a MicroCal PEAQ-ITC at a constant temperature of 25 °C. The reference cell was filled with ultrapure water. The stirring speed was set to 750 rpm. A preliminary injection of 0.4 µL was discarded to account for diffusion effects from the syringe tip. This was followed by a series of 12 identical injections of 2 µL each, spaced 150 seconds apart to allow the signal to return to baseline. The heat of dilution for each titrant was measured by injecting it into the assay buffer. This background signal was subtracted from the corresponding sample data during analysis.

Simulation details and methodology

Using Lipid21 force field [1], molecular dynamics simulations are performed using GROMACS 2021.7 software [2]. Long-range electrostatic interactions are treated with the particle mesh Ewald (PME) method [3] with 1.2 nm as the Coulomb cutoff, and the van der Waals (vdW) interactions are treated with the force-switching method [4], where the forces smoothly decayed to zero between 0.9 and 1.2 nm to reduce the cutoff noise. The LINCS algorithm [5] is used to apply the bond constraint related to hydrogen, and a dispersion correction is used for both energy and pressure. All the simulation systems are energy-minimized by 5000 steps steepest descent with a time step of 1 fs, and then undergo 1 ns of NVT and NPT pre-equilibration run using leap-frog MD integrator [6] with the non-water molecules restrained in their initial positions (force constant 1000 kJ/mol/nm^2) before launching a long time (20 ns) unrestrained production run with a time step of 2 fs. During all the simulations, temperature is kept constant at 298.15K by using the velocity rescaling (V-rescale) thermostat [7] (with τ_t = 1.0 ps), and pressure is kept at 1 bar by C-rescale semi-isotropic barostat (with τ_p = 0.5 ps)[8]. Results are visualized using VMD 1.9.3 [9] software.

Determination of Minimum Inhibitory Concentration (MIC)

Fresh bacterial colonies from an overnight agar plate were suspended in sterile saline (0.85% NaCl) to a density equivalent to a 0.5 McFarland standard, which corresponds to approximately 10^8 CFU/mL. This bacterial suspension was then diluted 1:150 in cation-adjusted Mueller-Hinton Broth (CAMHB) to achieve a final working inoculum of approximately 5-7 × 10^5 CFU/mL (OD_{600} = 0.16). A stock solution of the test compound (Cn-N-Me) was prepared in a suitable solvent at a high concentration. The final concentration of the solvent in the test wells did not exceed 1% (v/v), a level confirmed to not inhibit bacterial growth. A two-fold serial dilution of the compound was prepared directly in a sterile 96-well microtiter plate to create a concentration gradient. Briefly, 200 μL of CAMHB was dispensed into wells 2 to 12. Then, 100 μL of the compound stock solution, diluted in CAMHB to the highest test concentration (2048 μg/mL), was added to the first well (well A1). After thorough mixing, 200 μL was transferred from well A1 to well A2. This serial transfer was repeated consecutively from well to well down the column, resulting in a two-fold dilution series (from 1024 μg/mL to 1 μg/mL). A final 200 μL was discarded from the last well (well A12) to maintain equal volumes across all wells. After incubation, the MIC was determined visually as the lowest concentration of the compound that completely inhibited visible growth of the organism. Alternatively, the optical density at 600 nm (OD_{600}) was measured using a microplate reader to provide an objective endpoint. The MIC was defined as the lowest concentration that resulted in an OD_{600} equal to or less than that of the sterility control.

Agar Disk Diffusion Assay for Antibacterial Activity

Fresh bacterial colonies were suspended in sterile saline (0.85% NaCl), and the turbidity was adjusted to a 0.5 McFarland standard (approximately 1-2 × 10^8 CFU/mL). Sterile cotton swabs were used to evenly swab the entire surface of Mueller-Hinton Agar (MHA) plates in three directions to achieve a confluent lawn of bacterial growth. Using a sterile cork borer or a sterile pipette tip, a well (approximately 1 cm in diameter) was punched aseptically into the center of the solidified, inoculated agar plate. The agar plug was carefully removed using a sterile instrument. Using a micropipette, 300 μL of the test compound solution (C_{16}-N-Me or C_{16}-N-Na at a specified concentration,

typically 512 mg/mL) was carefully added into the well. The hydrolyzed product C_{16}-N-Na was tested at the same molar concentration as C_{16}-N-Me for a direct comparison. The plates were allowed to stand at room temperature for 10-15 minutes to permit the pre-diffusion of the compounds into the agar. The inoculated plates were incubated at 37 °C for 16-18 hours. After incubation, the diameter of the inhibition zone (the clear, circular area around the well where bacterial growth was completely inhibited) was measured to the nearest millimeter using a caliper or a ruler.

Assessment of Membrane Integrity by Nucleic Acid Leakage Using UV-Vis Spectroscopy

The membrane disruption activity of the model compounds (C_{16}-N-Me and its hydrolyzed product C_{16}-N-Na) against E. coli and S. aureus was evaluated by quantifying the release of intracellular nucleic acids, which absorb strongly at 260 nm. Both bacterial strains were cultured in Luria-Bertani (LB) broth at 37 °C with shaking until the mid-logarithmic growth phase (OD_{600} ≈ 0.6). The cells were harvested by centrifugation (5,000 × g, 10 min, 4 °C), washed twice, and resuspended in sterile phosphate-buffered saline (PBS, 1X, pH 7.4) to an OD_{600} of approximately 0.8 (standardized cell density). Added with C_n-N-R at a final concentration of 1024μg/mL. All samples were incubated at 37 °C for 2 hours with gentle shaking.After incubation, the samples were immediately centrifuged at 12,000 × g for 5 minutes at 4 °C to pellet the bacterial cells and any debris.The resulting supernatants were carefully collected and filtered through a 0.22 μm syringe filter to remove any remaining cells or large particles. The absorbance of the clarified supernatants was measured at 260 nm (A_{260}) using a UV-Vis spectrophotometer, with PBS used as the blank. The relative amount of nucleic acids leaked from the bacteria was directly proportional to the absorbance value at 260 nm. The data were presented as the mean A_{260} value from at least three independent experiments.

Scanning Electron Microscopy (SEM) for Observing Bacterial Morphology

The Both bacterial strains were cultured in Luria-Bertani (LB) broth at 37 °C with shaking until the mid-logarithmic growth phase. The cells were harvested by centrifugation (5,000 × g, 10 min), washed, and resuspended in fresh PBS. The bacterial

suspensions were treated with C16-N-Me at 128 μg/mL for 2 hours at 37 °C. Control groups included bacteria treated with an equimolar concentration of C16-N-Na and bacteria in PBS only (negative control). After treatment, the bacteria were immediately fixed by adding an equal volume of 2.5% glutaraldehyde (in 0.1 M PBS, pH 7.4) and incubating at 4 °C for 4-12 hours. The fixed bacterial pellets were washed with PBS and then dehydrated through a graded ethanol series (30%, 50%, 70%, 80%, 90%, and 100% ethanol) for 15 minutes at each concentration. The 100% ethanol step was repeated twice. A small volume of the dehydrated bacterial suspension in 100% ethanol was dropped onto a clean silica wafer and allowed to air dry in a desiccator. The dried samples were mounted on aluminum stubs and sputter-coated with a thin layer of gold-palladium to make them conductive for SEM imaging.

Bacteria staining

S. aureus was treated with C16-N-Me and CTAB each at its minimal inhibitory concentration for 30 min. After treatment, cells were stained with the propidium iodide, PI, for 15 min in the dark. Following staining, cells were immobilized on agarose pads and immediately examined under a fluorescence microscope or confocal laser scanning microscopy, CLSM. PI penetrated cells with compromised membranes and stained them red.

In Vitro Hemolysis Assay Using Porcine Red Blood Cells (pRBC)

Commercially obtained fresh liquid porcine red blood cells were used. The cell suspension was transferred to a centrifuge tube and washed three times with cold PBS by centrifugation (1,500 × g, 10 min, 4 °C) to remove the preservation solution. After reconstitution or washing, the porcine red blood cells were resuspended in PBS to prepare a 4% (v/v) working suspension. The test compounds (C_{16}-N-Me and C_{16}-N-Na) were dissolved in PBS and serially diluted to the desired concentrations (1 mM, 0.5 mM and 0.25 mM). 0.5 mL of each compound solution was mixed with 0.5 mL of the 4% pRBC suspension in a 1.5 mL microcentrifuge tube. This resulted in a final pRBC concentration of 2% (v/v) for the assay. The mixtures were gently vortexed and then incubated in a water bath at 37 °C for 1 hour. Negative Control (0% Hemolysis, 0.5 mL of PBS mixed with 0.5 mL of 4% pRBC suspension.) and Positive Control (100%

Hemolysis, 0.5 mL of 1% (v/v) Triton X-100 solution mixed with 0.5 mL of 4% pRBC suspension.) were included in each experiment. After incubation, all tubes were centrifuged at 3,000 × g for 5 minutes to pellet any intact pRBCs and cellular debris. The clear supernatant from each tube was then carefully transferred into a standard 1 cm pathlength quartz. The absorbance of the supernatants was measured at 540 nm (A_{540}) using a UV-Vis spectrophotometer, with PBS used as the blank to zero the instrument. The hemolysis percentage was calculated as: Hemolysis (%) = $[(A_{sample} - A_{negative\ control}) / (A_{positive\ control} - A_{negative\ control})] \times 100\%$.

Cell culture and cellular cytotoxicity evaluation

L929 cells were cultured in DMEM high-glucose medium supplemented with 10% FBS and 1% P/S. All cells were cultured at 37°C in a 5% CO_2 humidified chamber. The cytotoxicity assay was carried out using a CCK-8 assay. Typically, BEAS-2B cells were cultured into DMEM supplemented with 10% FBS and 100.0 μg/mL P/S, then cells were seeded in a 96-well plate and incubated for 24 h at 37 °C with 5% CO_2. Subsequently, fresh cell culture medium with different concentrations of Cn-N-R was added to the culture wells, and the cells were incubated for 24 h. After that, cells were washed with PBS. To perform the CCK-8 assay, the culture medium was removed after another 24 h, and the wells were washed with PBS three times. Then the culture medium containing the CCK-8 reagent (10.0 μL) was added, followed by incubation for 30 min at 37°C to allow the formation of formazan dye. Finally, the optical absorption of the formazan dye at 450 nm was measured on a plate reader.

Staining of live and dead cells

L929 cells were seeded onto Petri dishes and incubated overnight. Subsequently, cell culture mediums containing Cn-N-R (1.0 mM) were added to the wells to replace the previous cell culture medium. After 4 h incubation, the culture medium was removed and washed with PBS three times. Then the cells were treated with Calcein-AM/PI solutions (1 μM, PBS) for 30 min. After being washed by PBS three times, cells were observed by inverted fluorescence microscopy. (Calcein-AM: Ex/Em: 495 nm/520 nm, PI: Ex/Em: 530 nm/620 nm).

Detection of ROS

L929 cells were seeded onto glass-bottomed Petri dishes and incubated overnight, then the culture medium was replaced by the medium containing Cn-N-R (1.0 mM). After co-culturing for 2 h, the culture medium was removed and the cells were washed with PBS three times. Next, PBS containing 10.0 μM DCFH-DA was added to incubation for 20 min. After washing three times with PBS to adequately remove DCFH-DA, a laser scanning confocal fluorescence microscope was used to capture the fluorescence image of the cells. It should be noted that a positive control group was conducted by treating the cells with a ROS-positive simulator.

***In Vivo* safety experiments**

Six-week-old mice (female, C57BL/6) were supplied by Beijing Vital River Laboratory Animal Technology Co., Ltd., and housed in the Peking University Health Science Center, Department of Laboratory Animal Science. First, the mice were fasted for 12 h. Then mice were gavaged with 0.5 mL of aqueous Cn-N-R solutions at various concentrations using a gavage needle. Next, mice resumed eating after fasting for 2 h. On day 2, mouse feces were collected and extracted with water, and the extraction solution was tested by HPLC. On day 3, after eyeball blood sampling, the mice were sacrificed and the major organs were stained with hematoxylin and eosin (H&E) according to a standard procedure. All animal experiments were conducted in accordance with the protocols authorized by the Institutional Animal Care and Use Committee (IACUC) and in compliance with the legal requirements for laboratory animals in China. The experiments were carried out in conforming to the institutional guidelines established by the Laboratory Animal Research Center of Peking University (AAALAC unit number: 001249), which approved our experimental protocol and procedures.

Reference:

[1] Lipid21: Complex Lipid Membrane Simulations with AMBER. J. Chem. Theory Comput. 2022, 18, 3, 1726–1736.

[2] GROMACS: High performance molecular simulations through multi-level parallelism from laptops to supercomputers. SoftwareX. 2015, 1-2, 19-25.

[3] A smooth particle mesh Ewald method. J. Chem. Phys. 1995, 103, 8577-8593.

[4] New spherical-cutoff methods for long-range forces in macromolecular simulation. J. Comput. Chem. 1994, 15, 667-683.

[5] LINCS: A linear constraint solver for molecular simulations. J. Comput. Chem. 1997, 18, 1463-1472.

[6] Quiet high-resolution computer models of a plasma. J. Comput. Phys. 1974, 14, 148-158.

[7] Canonical sampling through velocity rescaling. J. Chem. Phys. 2007, 126, 014101.

[8] Pressure control using stochastic cell rescaling. J. Chem. Phys. 2020, 153, 114107.

[9] VMD: visual molecular dynamics. J. Mol. Graph. 1996, 14, 33-8.

Supplementary Figures.

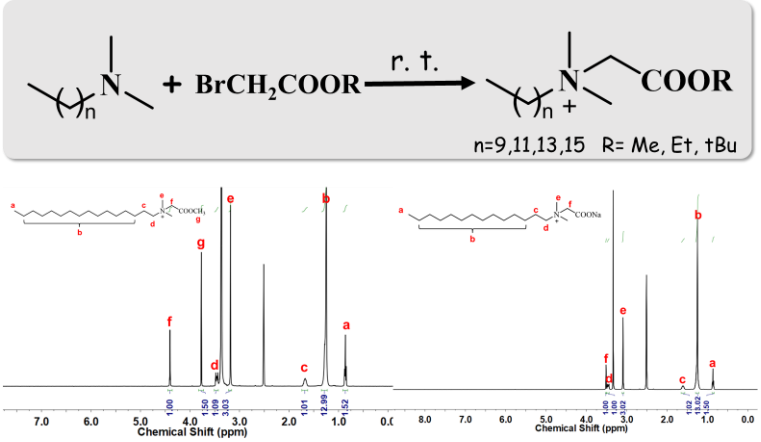

Figure S1. The synthesis method of ester based quaternary ammonium salts and partial nuclear magnetic spectrum.

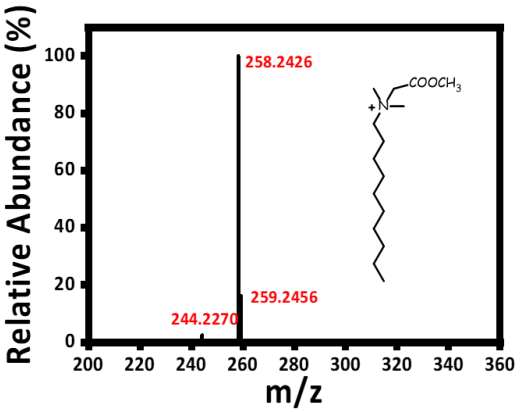

Figure S2. Mass spectrometry of C_{10}-N-Me. Only display peaks with relative abundance>1%.

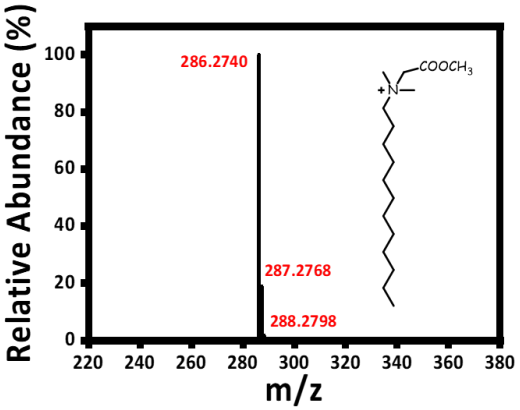

Figure S3. Mass spectrometry of C_{12}-N-Me. Only display peaks with relative abundance>1%.

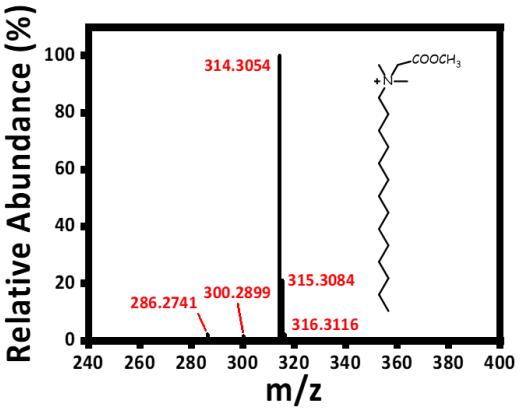

Figure S4. Mass spectrometry of C_{14}-N-Me. Only display peaks with relative abundance>1%.

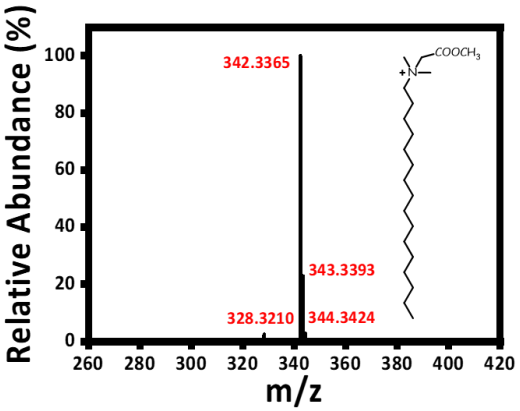

Figure S5. Mass spectrometry of C_{16}-N-Me. Only display peaks with relative abundance>1%.

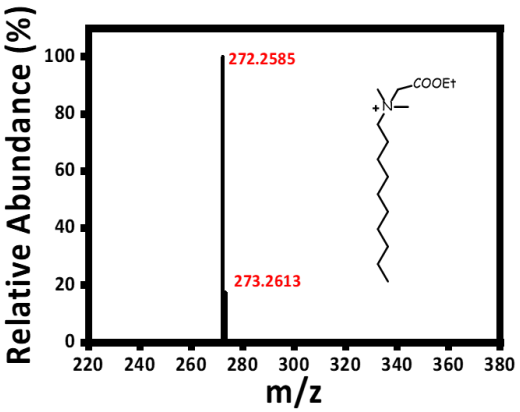

Figure S6. Mass spectrometry of C_{10}-N-Et. Only display peaks with relative abundance>1%.

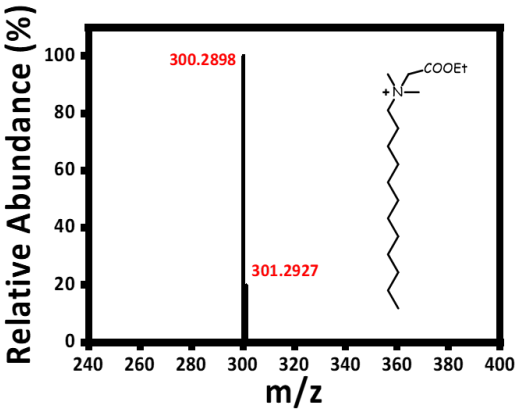

Figure S7. Mass spectrometry of C_{12}-N-Et. Only display peaks with relative abundance>1%.

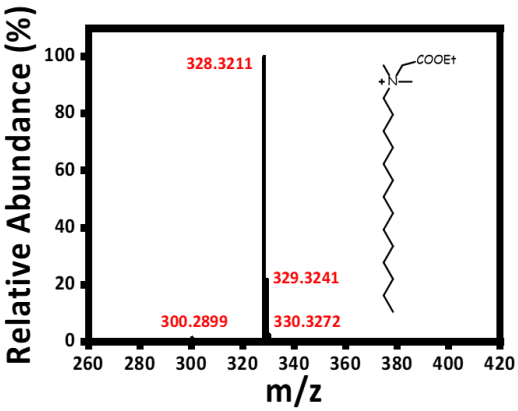

Figure S8. Mass spectrometry of C_{14}-N-Et. Only display peaks with relative abundance>1%.

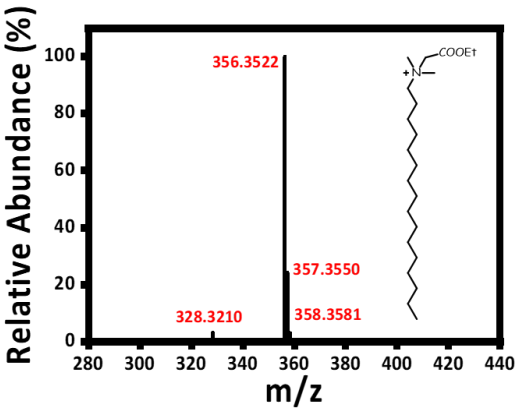

Figure S9. Mass spectrometry of C_{16}-N-Et. Only display peaks with relative abundance>1%.

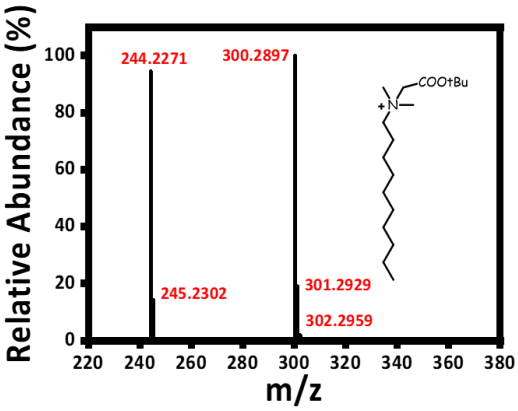

Figure S10. Mass spectrometry of C_{10}-N-tBu. Only display peaks with relative abundance>1%. When the R group is tBu, the molecule may be unstable due to high steric hindrance, making it more susceptible to fragmentation by bombardment. Therefore, there is a peak with m/z reduced by 57.0657 relative to the molecular peak.

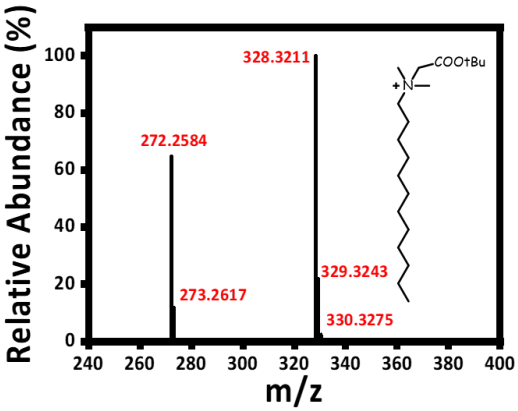

Figure S11. Mass spectrometry of C_{12}-N-tBu. Only display peaks with relative abundance>1%. When the R group is tBu, the molecule may be unstable due to high steric hindrance, making it more susceptible to fragmentation by bombardment. Therefore, there is a peak with m/z reduced by 57.0658 relative to the molecular peak.

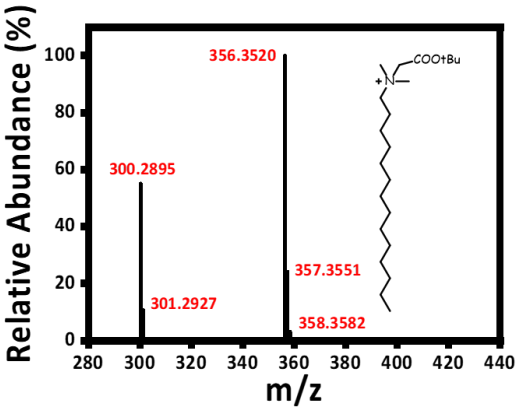

Figure S12. Mass spectrometry of C_{14}-N-tBu. Only display peaks with relative abundance>1%. When the R group is tBu, the molecule may be unstable due to high steric hindrance, making it more susceptible to fragmentation by bombardment. Therefore, there is a peak with m/z reduced by 57.0655 relative to the molecular peak.

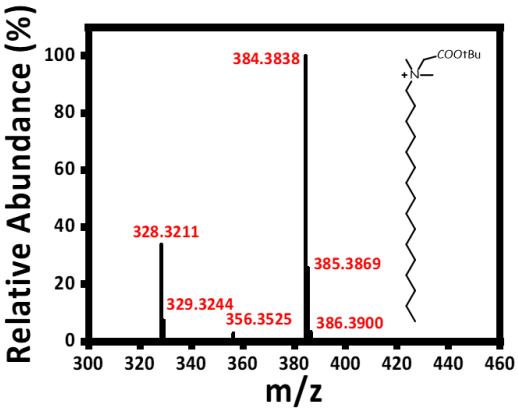

Figure S13. Mass spectrometry of C_{16}-N-tBu. Only display peaks with relative abundance>1%. When the R group is tBu, the molecule may be unstable due to high steric hindrance, making it more susceptible to fragmentation by bombardment. Therefore, there is a peak with m/z reduced by 57.0656 relative to the molecular peak.

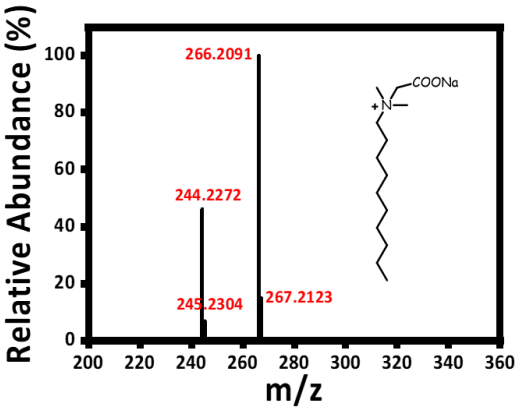

Figure S14. Mass spectrometry of C_{10}-N-Na. Only display peaks with relative abundance>1%. When the R group is Na, there is an ionic bond between Na and carboxyl, which has a low bond energy and is more easily bombarded into fragments. Therefore, there is a peak with m/z reduced by 22.9851 relative to the molecular peak.

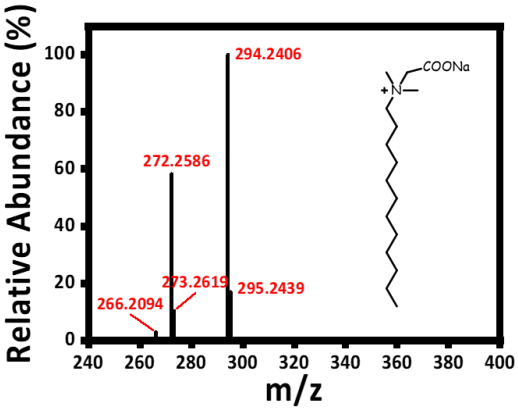

Figure S15. Mass spectrometry of C_{12}-N-Na. Mass spectrometry of C_{10}-N-Na. Only display peaks with relative abundance>1%. When the R group is Na, there is an ionic bond between Na and carboxyl, which has a low bond energy and is more easily bombarded into fragments. Therefore, there is a peak with m/z reduced by 22.9853 relative to the molecular peak.

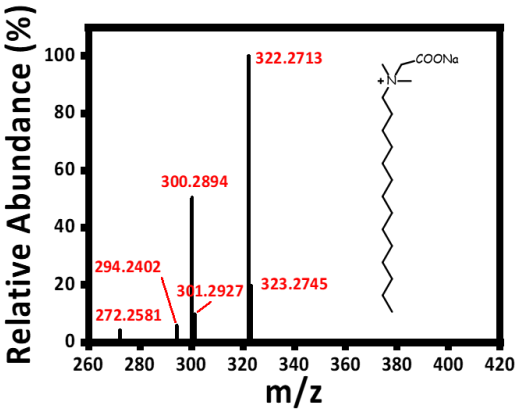

Figure S16. Mass spectrometry of C_{14}-N-Na. Mass spectrometry of C_{10}-N-Na. Only display peaks with relative abundance>1%. When the R group is Na, there is an ionic bond between Na and carboxyl, which has a low bond energy and is more easily bombarded into fragments. Therefore, there is a peak with m/z reduced by 22.9851 relative to the molecular peak.

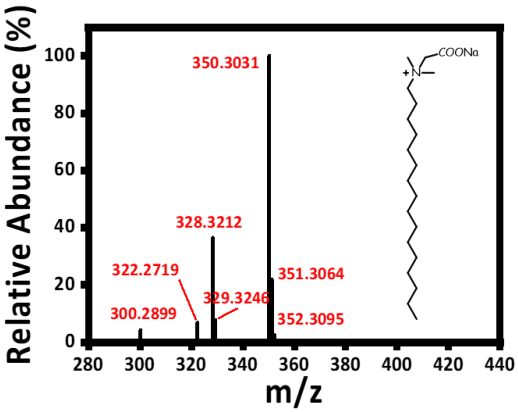

Figure S17. Mass spectrometry of C_{16}-N-Na. Mass spectrometry of C_{10}-N-Na. Only display peaks with relative abundance>1%. When the R group is Na, there is an ionic bond between Na and carboxyl, which has a low bond energy and is more easily bombarded into fragments. Therefore, there is a peak with m/z reduced by 22.9849 relative to the molecular peak.

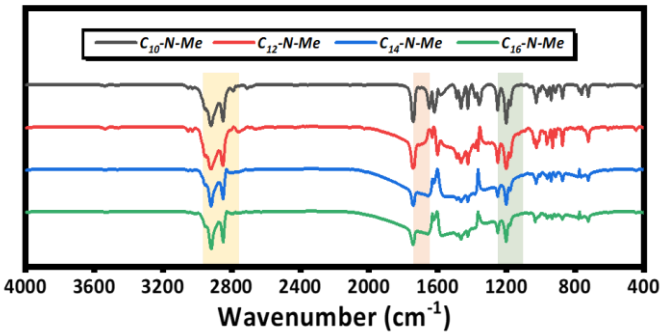

Figure S18. Fourier transform infrared spectra of ester quaternary ammonium salts with different chain lengths when R is methyl. Fourier transform infrared spectra of ester quaternary ammonium salts with different chain lengths when R is methyl. There are widely distributed stretching vibration peaks of C-H around 2900 cm^{-1}, indicating long alkyl chains. C=O stretching vibration occurs at around 1700 cm^{-1}

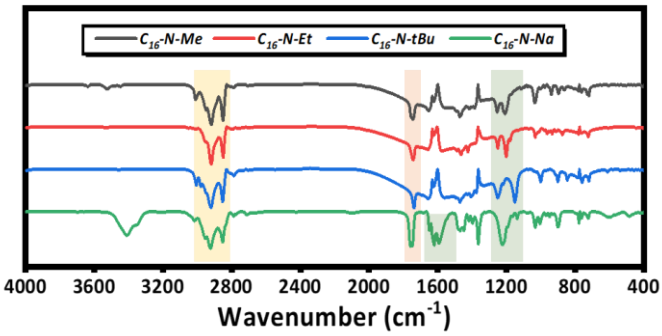

Figure S19. Fourier transform infrared spectra of different R bases when chain length n=16. Fourier transform infrared spectra of different R bases when chain length n=16. Except for C_{16}-N-Na, which exhibits symmetric and antisymmetric stretching vibrations of C-O-C at around 1200 cm^{-1}, it indicates the presence of ester groups. C_{16}-N-Na exhibits a wider peak of water hydroxyl stretching vibration at 3400 cm^{-1}, indicating stronger water absorption capacity.

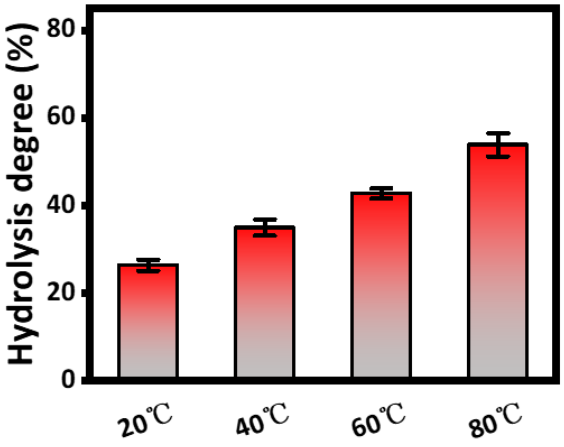

Figure S20. The hydrolysis extent of Ester-QACs under different temperature (n=16, R=Me, pH=7.0, t=24 h)

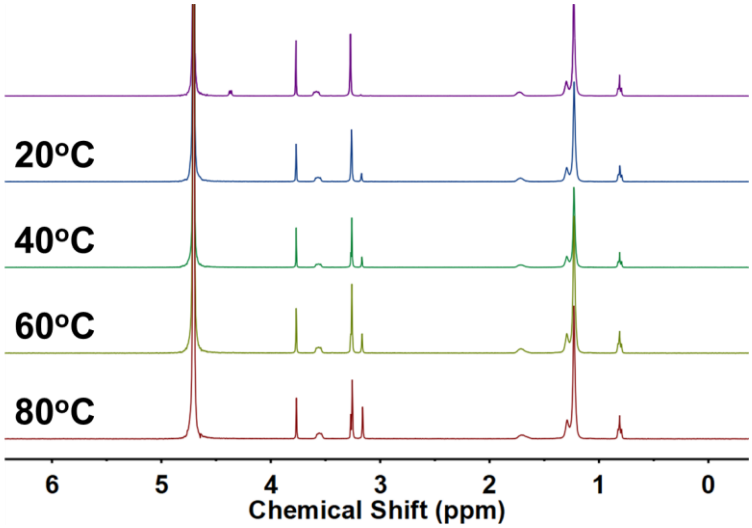

Figure S21. ^{1}H NMR spectra of hydrolysis of Ester-QACs at different temperatures (n=16, R=Me, pH 7.0, 24 h).

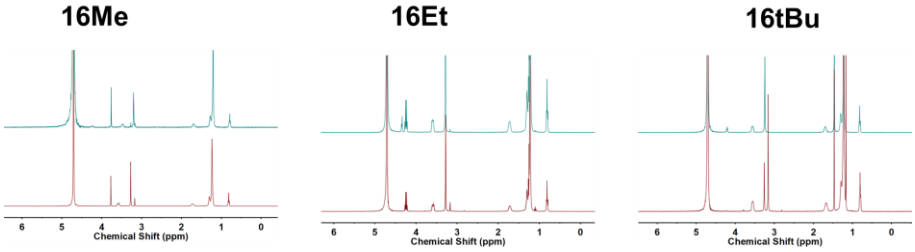

Figure S22. ^{1}H NMR spectra of hydrolysis of Ester-QACs at different substituents (R group) (n=16, pH 7.0, 24 h, 40°C).

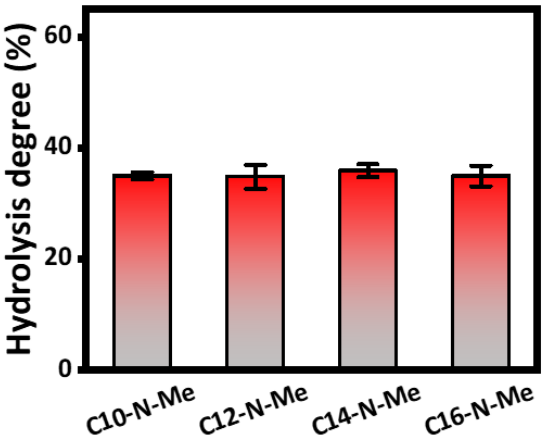

Figure S23. [1]H NMR spectra of hydrolysis of Ester-QACs at different carbon chain lengths (n) (R=Me, pH 7.0, 24 h, 40°C).

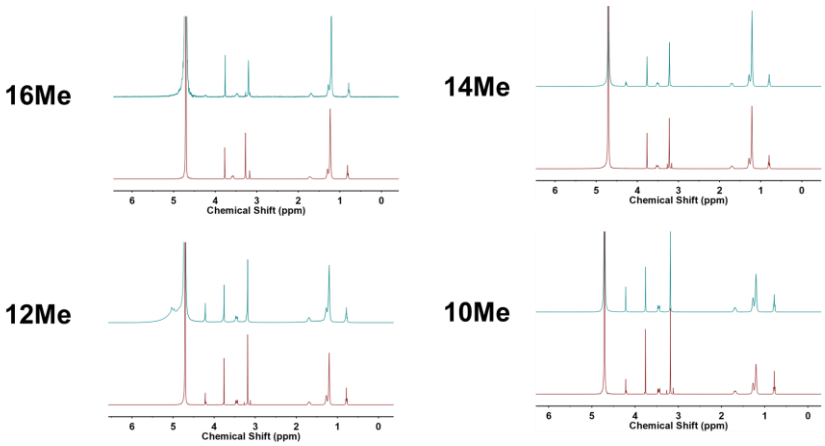

Figure S24. [1]H NMR spectra of hydrolysis of Ester-QACs at different carbon chain lengths (n) (R=Me, pH 7.0, 24 h, 40°C).

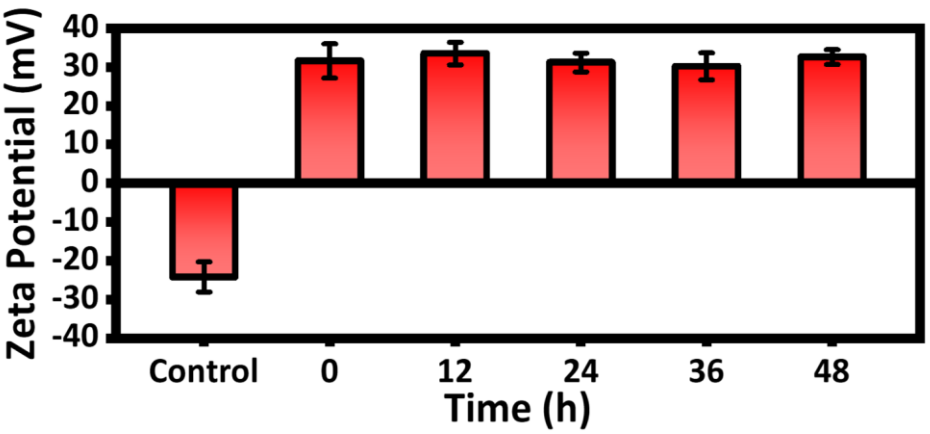

Figure S25. Zeta potential of S. aureus treated with CTAB incubated in aqueous solution for different durations.

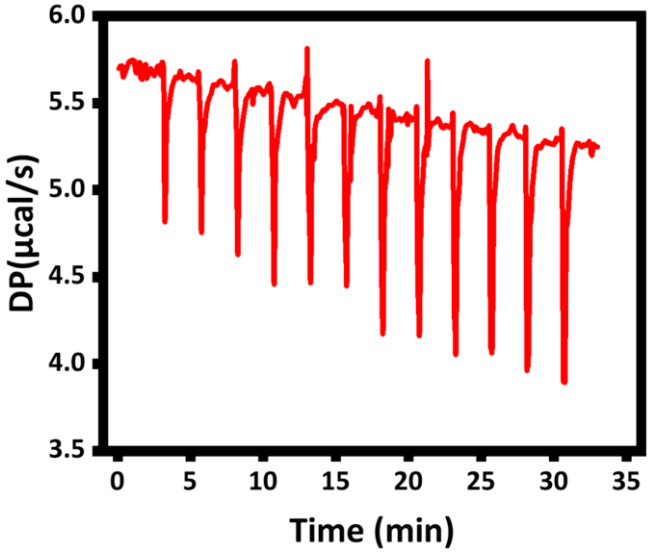

Figure S26. ITC profiles of S. aureus membrane vesicles titrated with CTAB.

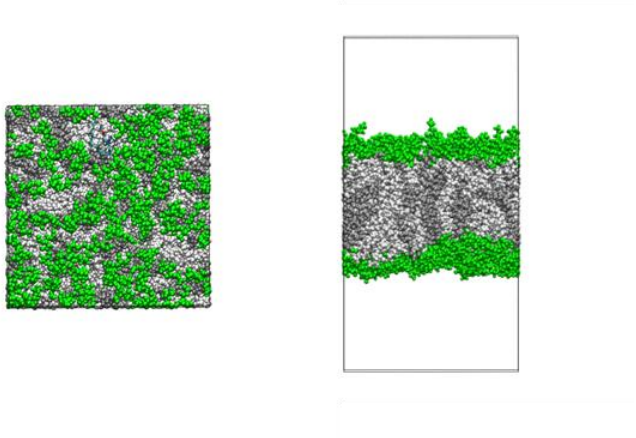

Figure S27. Top view (left) and front view (right) of molecular dynamics simulation of the interaction between C_{16}-N-Me and cell membrane.

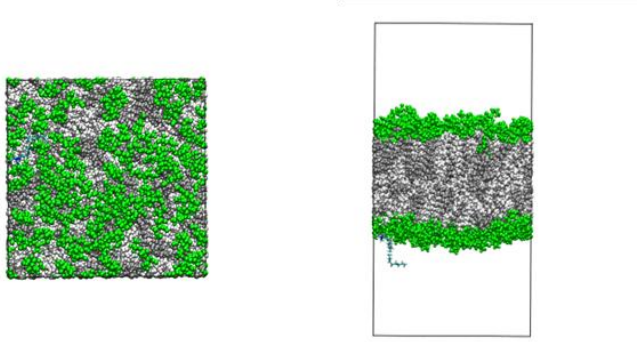

Figure S28. Top view (left) and front view (right) of molecular dynamics simulation of the interaction between C_{16}-N-Na and cell membrane.

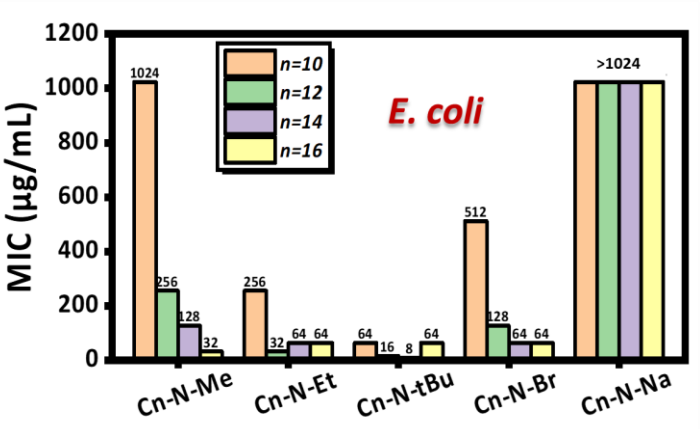

Figure S29. Minimum inhibitory concentration (MIC) of Ester-QACs and conventional QACs against E. coli.

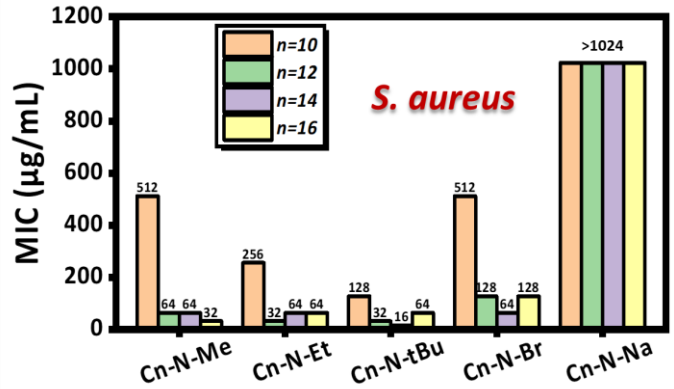

Figure S30. Minimum inhibitory concentration (MIC) of Ester-QACs and conventional QACs against S. aureus.

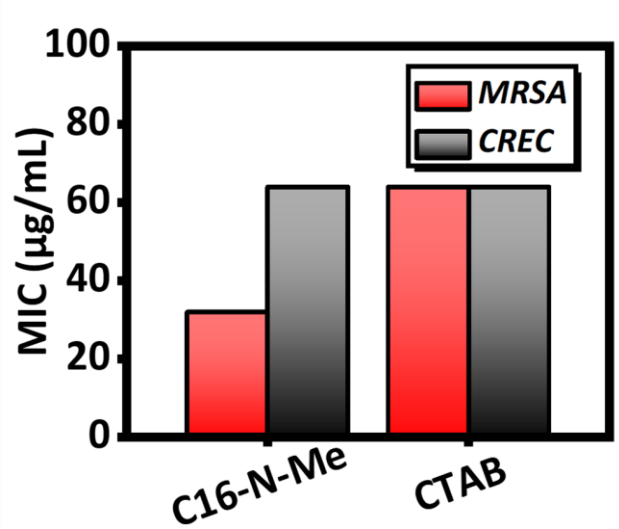

Figure S31. MIC of CTAB and C16-N-Me against drug-resistant bacteria.

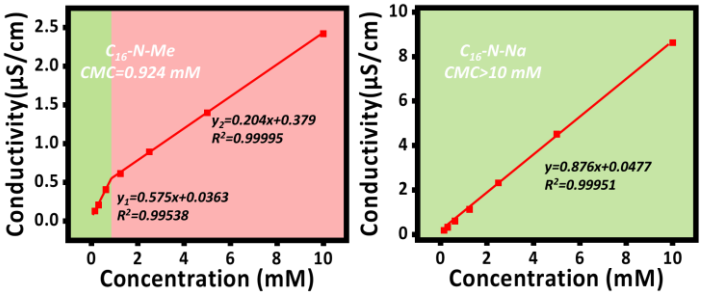

Figure S32. The conductivity of C_{16}-N-Me (left) and C_{16}-N-Na (right) varies with concentration. Within the tested concentration range, the critical micelle concentration (CMC) of C_{16}-N-Na did not appear, while the CMC of C_{16}-N-Me was 0.924 mM (approximately 400 μ g/mL)

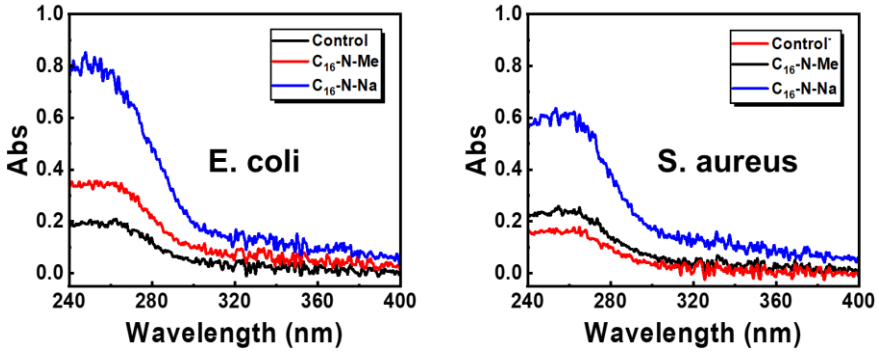

Figure S33. UV visible absorption spectra of the supernatant after drug treatment of E. coli (left) and S. aureus (right).

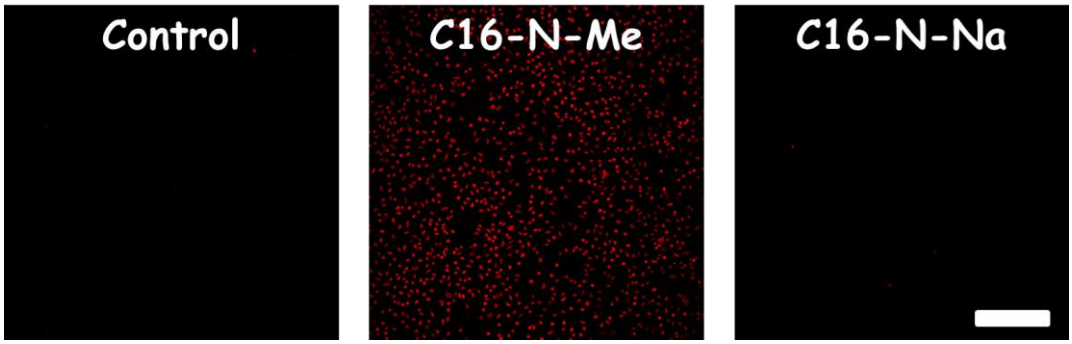

Figure S34. PI staining after treating S. aureus with C16-N-Me and C16-N-Na.. Scale bars, 250 μm.

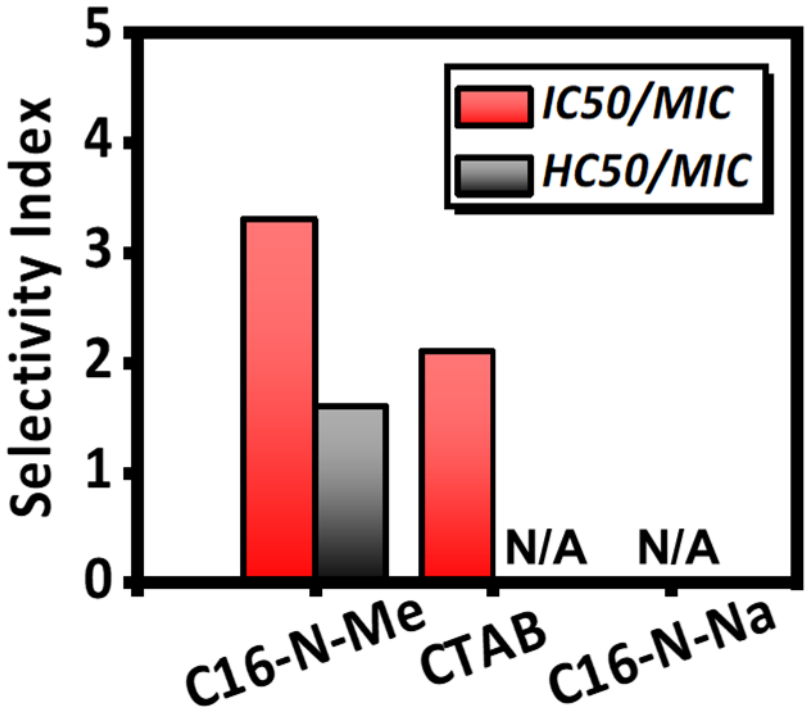

Figure S35. The selectivity index of hemolysis and cytotoxicity relative to antibacterial activity.

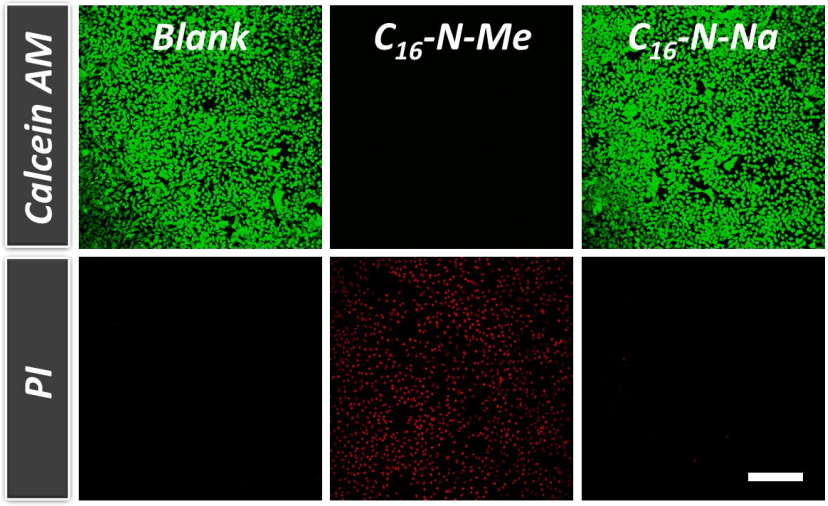

Figure S36. Live/Dead staining (green: live cells; red: dead cells) of L929 cells confirming the low toxicity of C16-N-Na. Scale bars, 250 μm.

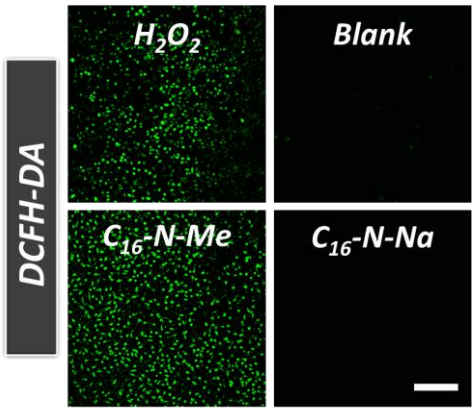

Figure S37. Intracellular ROS detection by DCFH-DA. C16-N-Me induces significant ROS generation, while C16-N-Na does not. Scale bars, 250 μm.

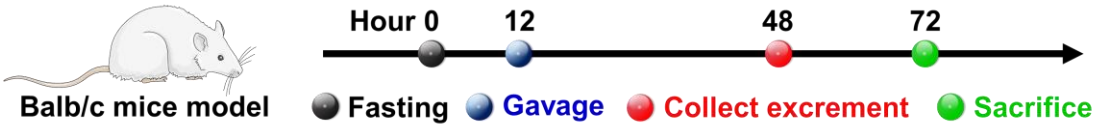

Figure S38. Schematic timeline of the mouse gavage experiment.

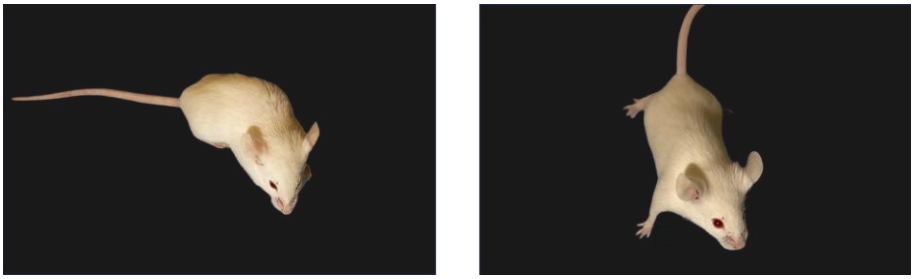

Figure S39. Representative photographs of murine behavior subsequent to the gavage of C16-N-Me (left) and C16-N-Na (right).

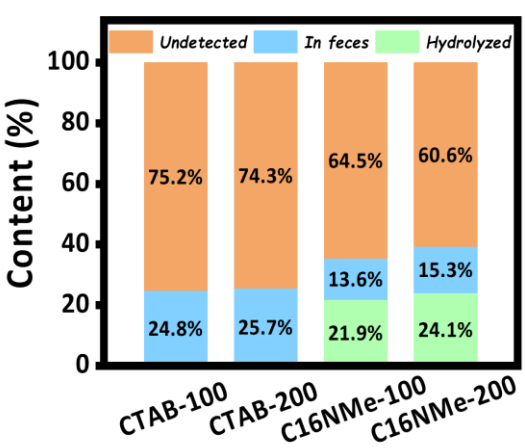

Figure S40. Content of fecal extracts showing the metabolic fate of CTAB (intact recovery) and C16-N-Me (partially hydrolyzed to C16-N-Na). (n=6 mice per group).

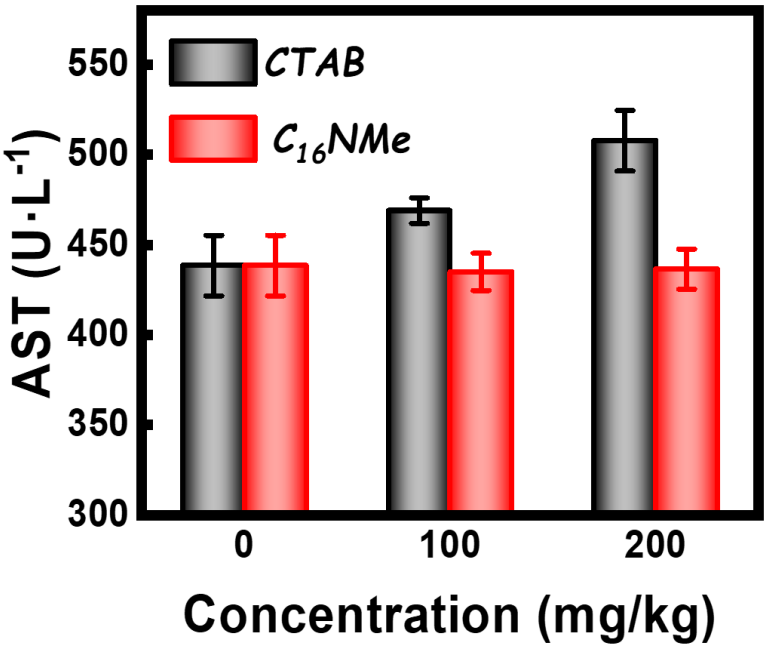

Figure S41. The content of serum biochemical indicator AST in serum. n=6 mice per group.

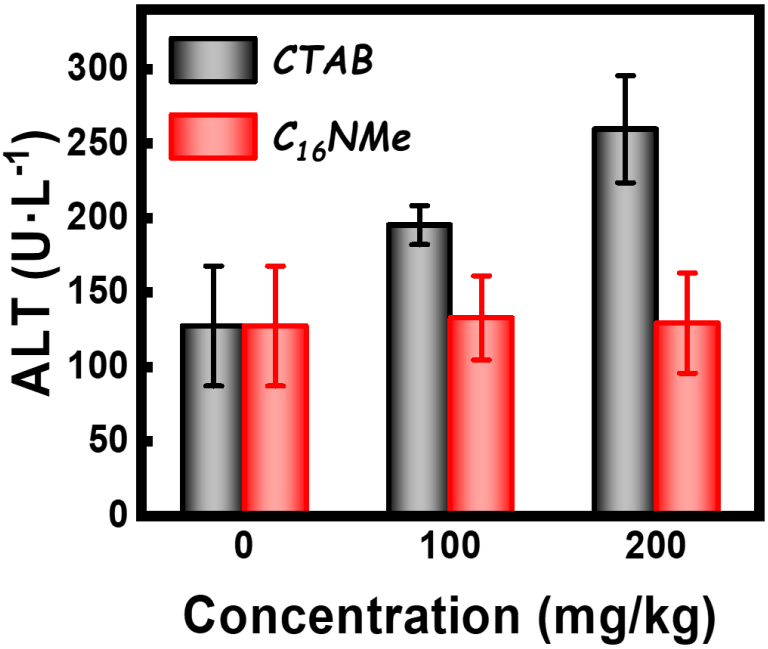

Figure S42. The content of serum biochemical indicator ALT in serum. n=6 mice per group.

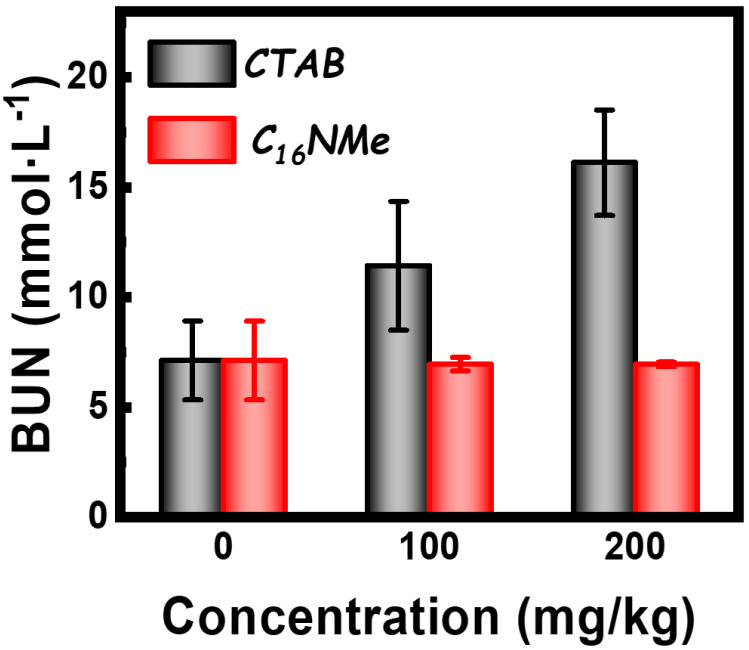

Figure S43. The content of serum biochemical indicator BUN in serum. n=6 mice per group.

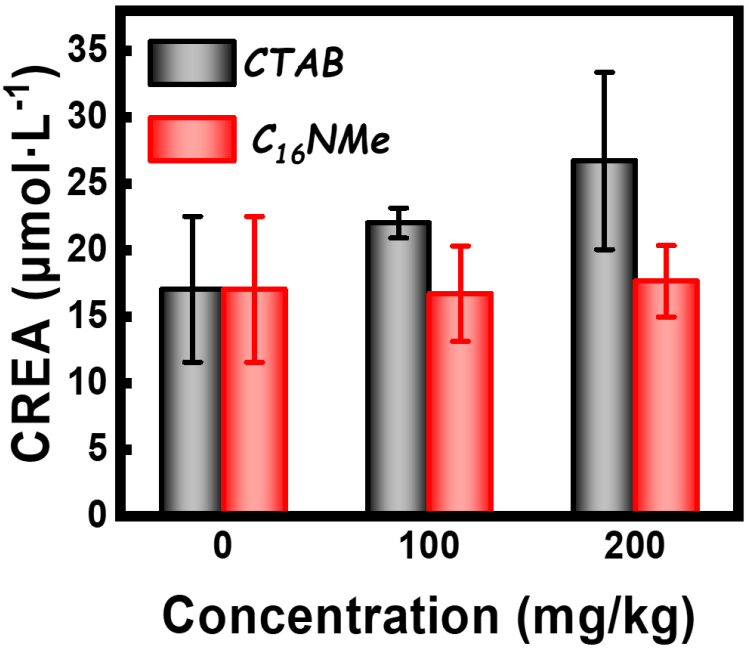

Figure S44. The content of serum biochemical indicator CREA in serum. n=6 mice per group.

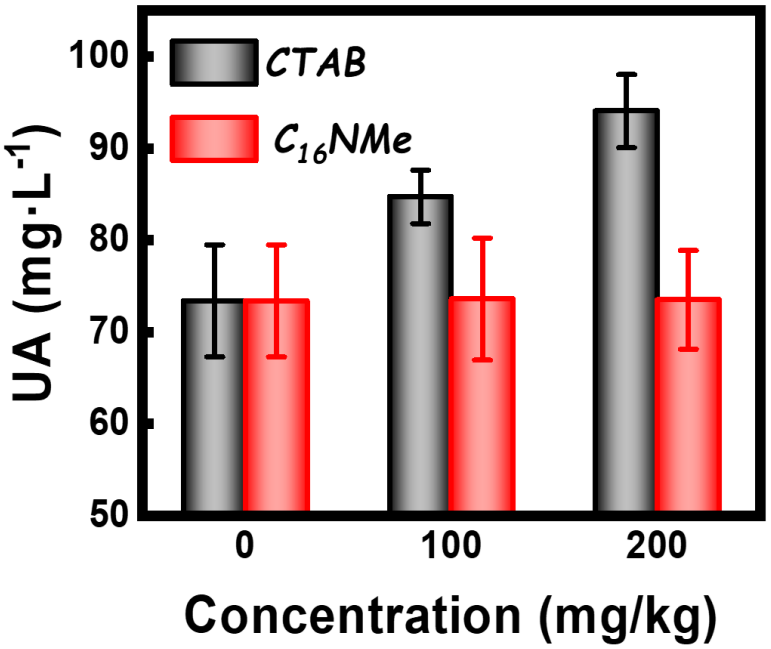

Figure S45. The content of serum biochemical indicator UA in serum. n=6 mice per group.